npj | sustainable agriculture

Article

https://doi.org/10.1038/s44264-026-00135-y

Breeding changes water use of winter wheat across Europe

Dominik Behrend[1] ✉, Thuy Huu Nguyen[1], Juan C. Baca Cabrera[2], Josef Baumert[3], Clara Oliva Gonçalves Bazzo[1,4], Dylan H. Jones[5], Guillaume Lobet[2,6], Sabine J. Seidel[1,7], Amit Kumar Srivastava[8], Hugo Storm[3], Jan Vanderborght[2], Frank Ewert[1,8] & Thomas Gaiser[1]

Breeding has altered wheat physiology substantially. While physiological improvements boosted grain yields, there is still limited understanding of how this affected agricultural water use on a continental scale. We employed a crop model, calibrated for a historical (released 1895) and a modern (released 2002) German winter wheat cultivar, across Europe for a period of 30 years to compare changes in transpiration. Throughout all locations and the simulation period, the modern cultivar transpired significantly less water (−17%) than the historical cultivar. Cultivar differences in transpiration were more pronounced in southern Europe. Over the whole 30-year period, an upward trend in transpiration was observed for both cultivars. Transpiration between cultivars was closely linked to higher leaf area index values. Root physiology was crucial, especially in dry regions. The findings underscore the need to incorporate cultivar-specific water use characteristics into large-scale assessments of land-atmosphere interactions and water use projections of agricultural lands.

Wheat (*Triticum aestivum* L.) is among the most dominant crops in Europe, covering large shares of the EU land area[1]. Over the past decades, winter wheat yields have increased substantially both in Europe and globally. In western Europe (here defined as Austria, Belgium, Denmark, France, Germany, Ireland, the Netherlands, Switzerland and the United Kingdom), already one of the most efficient cereal production regions globally, wheat yields significantly increased from an average of 4.6 t ha^{-1} during the period of 1964–1990 to 7.2 t ha^{-1} during the period of 1993–2017[2]. These increases in yields have been mainly attributed to a combination of improved management practices such as enhanced fertilizer usage, disease control, and advances in breeding[3,4]. A recent multi-environment study over six consecutive years and nine crop management scenarios with 191 winter wheat cultivars released between 1963 and 2016, showed that 48% of the grain yield improvements can be explained by the breeding progress alone[5].

The major breeding contribution to increasing grain yields have been attributed to the optimization of the harvest index, defined as the ratio of grain yield to aboveground biomass, which led to an increased partitioning of biomass to the grain[6,7]. Other major improvements have been related to the phenology, with modern cultivars reaching physiological maturity earlier than historic cultivars[8], and to the canopy architecture to enhance light interception[9], resulting in smaller but erect flag leaves that allow for a deeper light penetration into the canopy[10]. Despite extensive research on yield improvements due to advances in cultivars, relatively little attention has been paid to the understanding of how cultivar-specific physiological differences affect transpiration and agricultural water use.

Among the advances in breeding that increased grain yields during the past decades, changes in canopy architecture and leaf area index (LAI) are likely to have the closest link to transpiration. Similarly, a change in the biomass partitioning between different organs, leading to a higher percentage of vegetative tissues, likely also increases transpiration. Phenology, on the other hand, is directly related to the length of the growth period and therefore lengthens or shortens the transpiration duration. Besides the impacts of breeding on grain yields, it is likely that modern varieties have also undergone unintentional selection for root traits[11], another key driver of water uptake and transpiration. Recent studies have shown that root architectural traits such as the root system size, the number of roots, the root angle, the rooting depth and the biomass partitioned to roots have been affected by breeding during the past decades[12–16]. In a combined approach of field phenotyping, root-pressure chamber measurements and functional structural plant modeling, Baca Cabrera et al.[15] showed for a set of six

[1]Institute of Crop Science and Resource Conservation (INRES)—Crop Science Group, University of Bonn, Bonn, Germany. [2]Institute of Bio-and Geosciences, Agrosphere (IBG-3), Forschungszentrum Jülich GmbH, Jülich, Germany. [3]Institute for Food and Resource Economics, University of Bonn, Bonn, Germany. [4]Institute of Crop Science and Resource Conservation (INRES)—Agro-Ecological Modeling Group, University of Bonn, Bonn, Germany. [5]Leibniz Institute of Plant Genetics & Crop Plant Research (IPK), OT Gatersleben, Seeland, Germany. [6]Earth and Life Institute, UC-Louvain, Louvain-la-Neuve, Belgium. [7]Institute of Organic Farming, Department of Agricultural Sciences, BOKU University, Vienna, Austria. [8]Leibniz Centre for Agricultural Landscape Research (ZALF), Müncheberg, Germany. ✉e-mail: dbehrend@uni-bonn.de

German winter wheat cultivars spanning a breeding history from 1896 to 2002, found a significantly lower root hydraulic conductance in modern varieties[15]. Those findings imply that breeding may have unintentionally favored cultivars that follow a more conservative water uptake strategy, which causes them to take up less water.

Studies that have directly compared transpiration rates also report a significant difference among cultivars. Schoppach and Sadok[17] investigated transpiration rates as a response to vapor pressure deficit (VPD) and soil drying of different elite wheat varieties in Australia and observed a substantial genetic variability. In a larger experiment under greenhouse conditions, Moritz et al.[18] observed a significant effect of genotype on cumulative transpiration and transpiration efficiency among 79 tested modern elite western European genotypes. Comparable results were also reported by Huang et al.[19], who compared two Chinese varieties. When comparing modern and historic Australian winter wheat varieties, Siddique et al.[20] also found a trend towards a lower water usage and a higher water use efficiency in modern varieties. While studies that suggest differences between genotypes in transpiration exist, studies that compare differences in water use characteristics between genotypes on field scales are scares, likely due to the challenges associated with the measurements of transpiration on a canopy scale under field conditions. Given the importance of wheat as a major land cover in Europe, such cultivar changes have potential to impact continental water cycles. Similar effects of other agricultural management interventions like the consideration of irrigation on water fluxes and hydrological cycles have already been shown in previous studies[21,22]. Sacks et al.[23], for example, showed that the consideration of irrigation in land surface models can increase canopy transpiration over all land areas by 0.579%. While only ~2.5% of the global land area is equipped for irrigation[21], genetic changes due to breeding, like the implementation of dwarf wheat varieties during the green revolution, have affected all agricultural areas. It is therefore important to assess possible implications of genetic variations on a continental scale, to capture feedbacks between agricultural management and continental water fluxes in crop and land surface models.

Until recently, most land surface models did not consider physiological differences even between crops, simulating most crops using basic parameters of unmanaged C3 or C4 grasses[24]. In recent years, more effort has been put into a detailed representation of croplands, for example, by incorporating the crop model Integrated Biosphere Simulator (IBIS)[25], to the Community Land Model (CLM) Version 4, 4.5 and 5[26], or by improving the global representation of crops in the Joint UK Land Environment Simulator (JULES)[27].

Recent model improvements in CLM, i.e., inclusion of root system and plant hydraulic conductance in the simulation of root water uptake[28], or the implementation of parameters for root crops such as potato and sugar beet[29], indicate that the work to improve the representation of processes in agricultural lands is ongoing. Those inclusions of process details might allow modern land surface models to also capture genetic differences between cultivars, which until now have not been considered in land surface models. In a first approach to assess spatial differences in agricultural management, Rabin et al.[30] added observation-based diversified crop planting/sowing dates for different locations and crops in a worldwide simulation, observing a significant change in the simulated global irrigation demand by 15%. Although spatial variability in sowing dates is an important parameter for the simulation of crop growth, as discussed above, physiological differences between cultivars go beyond phenology and include differences in canopy structure and root hydraulic properties.

The aim of this work is therefore to evaluate how differences between historic and modern winter wheat cultivars have affected transpiration rates on a continental scale. To do this, we calibrated the crop model SIMPLACE<LintulCC2> (LintulCC2) using experimental data of two winter wheat cultivars. As part of the SIMPLACE modeling framework[31], LintulCC2 has been specifically developed to simulate soil-crop-atmosphere interactions. It has already been applied under a wide range of soil and management conditions[32], and different climate and soil conditions across Europe[33]. While it lacks the optional connection to an atmospheric model like most land surface models, it contains less overhead in terms of processes that are not required for the simulation of crop growth, and is easier to apply. The two German winter wheat cultivars used for calibration were the historical cultivar S. Dickkopf (released 1895) and the more modern cultivar Tommi (released 2002). Both cultivars were among the most grown cultivars of their times in Germany and previously investigated regarding their yield traits by Ahrends et al.[3] and Hernández-Ochoa et al.[34]. Physiological traits of both cultivars, among them the leaf area index development throughout their growth period, transpiration and biomass partitioning, were previously investigated in the experiments by Behrend et al.[35]. Root traits and root hydraulic conductance was further investigated by Baca Cabrera et al.[15] and Jones et al.[16]. The model was upscaled to the European domain on a 3 × 3 km grid for the period of 1990–2020 to answer the following questions: (1) Do physiological differences between winter wheat cultivars affect crop transpiration on a continental scale? (2) Were cultivar differences in transpiration constant over time and are they affected by the climate zone? (3) What are the main reasons for cultivar differences at EU scale and in different climate zones?

Results

Model calibration and validation at field scale

Model calibration for above-ground biomass data of the growing season 2023/2024 resulted in rRMSE values of 0.25 and 0.22, along with d-index values of 0.96 and 0.97 for the modern cultivar Tommi and the historic cultivar S. Dickkopf, respectively (Fig. 1). In both cultivars, these values were influenced by biomass overestimations in two out of six observations. When focusing only on values of above-ground biomass at harvest, rRMSE values of 0.09 for Tommi and 0.04 for S. Dickkopf were observed. The best fit of all variables was achieved in the calibration results of the LAI with rRMSE values of 0.06 and 0.1 and d-index values of 0.99 and 0.98 for Tommi and S. Dickkopf, capturing LAI dynamics throughout the season almost perfectly for Tommi and slightly underestimating the LAI after anthesis in S. Dickkopf. Comparing the simulation results of the canopy transpiration with the observations of the sap-flow sensors, rRMSE values of Tommi showed a value of 0.39 and of S. Dickkopf a value of 0.35, with good d-index values of 0.91 for Tommi and 0.84 for S. Dickkopf. Compared to the observations, the model captured transpiration well before the grain filling phase but tended to slightly underestimate transpiration during grain filling, especially for the historic cultivar. Validation of total above-ground biomass simulations for the growing season 2022/2023 showed rRMSE and d-index values similar to the calibration, reaching rRMSE values of 0.2 and d-index values of 0.97 for both cultivars (Fig. 2). This was again affected by an underestimation of observations in two sampling dates, while the harvest aboveground biomass at the end of the season reached rRMSE values of 0.16 for Tommi and 0.11 for S. Dickkopf, indicating a slight underestimation of observed values. Validation results of the LAI, with rRMSE values of 0.19 and 0.17 for Tommi and S. Dickkopf, were close to the calibration. D-index values of 0.9 and 0.95 showed that the model was still able to capture the LAI dynamics of both cultivars throughout the growing season well.

Comparing simulations with observations across Europe

Comparisons of simulations of day of the year (DOY) of anthesis from the simulation results of the modern cultivars with observations at the sites with observed anthesis DOY in Germany and Italy showed an rRMSE value of 0.1 and a d-index of 0.77 (Fig. 3a). When looking at the two countries individually, results fit best with observations from Italy, with an rRMSE of 0.02 and a MAE of 2.67. Comparisons of simulated DOY of anthesis with observations from Germany showed an rRMSE of 0.14 and a MAE of 18.8, overestimating the DOY of anthesis in Germany.

Such differences between countries were also observed in the comparisons of the simulated LAI at anthesis and the remotely sensed LAI (Fig. 3b). Results over all years and countries showed rRMSE of 0.26 and a MAE of 0.63, showing a general overestimation of LAI. When looking at

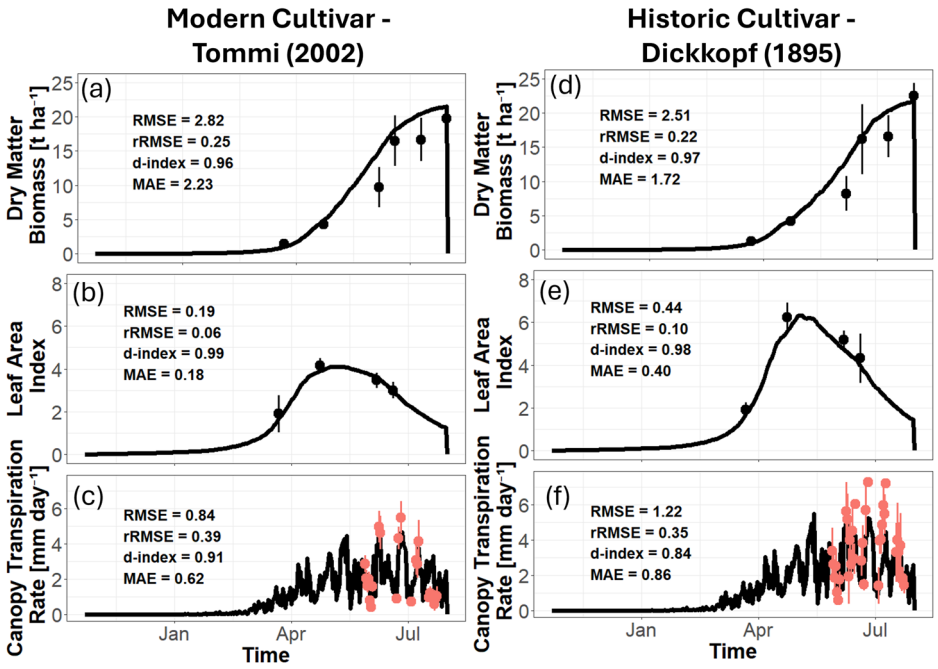

Fig. 1 | Crop model calibration on the field scale. Crop model calibration results of the calibration of above ground dry matter biomass (t ha^{-1}; **a**, **d**), leaf area index (**b**, **e**) and canopy transpiration rates (mm day^{-1}; **c**, **f**) of the winter wheat cultivars Tommi (released 2002, **a**–**c**) and S. Dickkopf (released 1895, **d**–**f**). Lines indicate model simulation results, points indicate mean observations of the respective outputs with standard deviations (see Table S1 for number of measurements of each variable), measured in the year 2024. Metrics of model fit presented are root mean square error (RMSE), relative root mean square error (rRMSE), Willmott's index of agreement (d-Index), mean absolute Error (MAE).

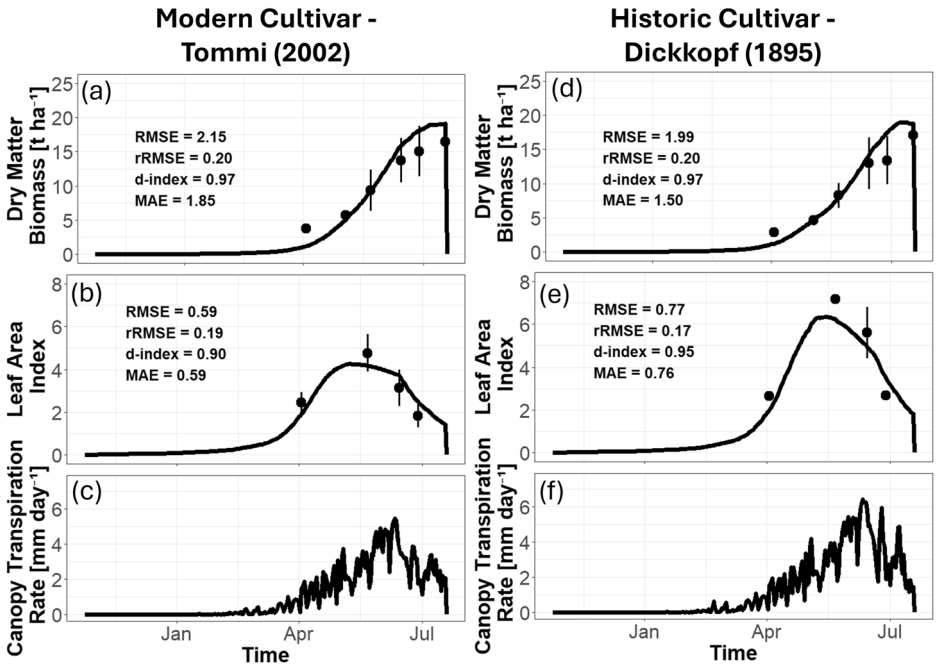

Fig. 2 | Crop model validation on the field scale. Crop model validation results of total above ground dry matter biomass (t ha^{-1}; **a**, **d**), leaf area index (**b**, **e**) and canopy transpiration rates (mm day^{-1}; **c**, **f**) of the winter wheat cultivars Tommi (released 2002, **a**–**c**) and S. Dickkopf (released 1895, **d**–**f**). Lines indicate model simulation results, points with indicate mean observations of the respective parameters with standard deviations, measured in the year 2023. Metrics of model fit presented are root mean square error (RMSE), relative root mean square error (rRMSE), Willmott's index of agreement (d-Index), mean absolute Error (MAE).

specific countries, results show that simulations in Italy fit well with the observations, showing rRMSE values of 0.04 and MAE of 0.11, while results in Germany show rRMSE values of 0.39 and MAI of 1.04.

Cultivar effects on transpiration at a continental scale

Transpiration difference across Europe over 30 years showed a reduction by −17% from the historic to the modern cultivar, with mean seasonal transpiration values of 266.5 ± 41.2 for the modern cultivar and mean seasonal transpiration values of 319.9 ± 32.2 (mm m^{-2} growing season^{-1}) for the historic cultivar. Maps with mean transpiration values of each grid cell over the whole timeframe from 1990 to 2020 for both cultivars and their difference show the highest transpiration values in central Spain and southern France (Fig. 4). Differences between cultivars are largest for southern Spain, Italy and Greece, according to the model, while smallest differences were observed in southern Germany and central Spain (Fig. 4).

When comparing the transpiration values of the two cultivars in different Köppen-Geiger climate zones, largest mean yearly transpiration values for both cultivars, with values of 318 ± 63 and 373 ± 62.8 mm for the modern and historic cultivar, respectively, can be found in the climate zone Csb, which is a Mediterranean climate zone characterized by a warm summer (Fig. 5). The lowest average simulated transpiration values were observed in the subarctic climate zone Dfc, with mean yearly transpiration values of 244 ± 26.4 mm for the modern and 300 ± 26.3 mm for the historic cultivar. Differences between the two cultivars were significant in all the climatic regions ($p < 0.001$). Largest simulated cultivar differences were found in the climate zone Csa, with a difference of −34%. These differences

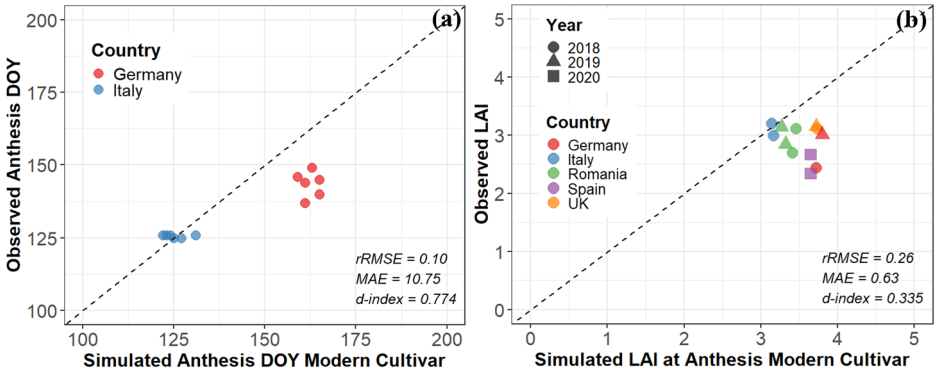

Fig. 3 | Crop model validation of LAI across Europe. Comparison of measured and simulated **a** anthesis day of the year (DOY) and **b** leaf area index (LAI) at anthesis. Anthesis DOY observations were obtained from three phenology stations in Brandenburg, Germany with two growing seasons (2017–2018 and 2018–2019) and from four locations in Italy with the one growing season (2017–2018). LAI observations points are mean values for winter wheat fields within a Sentinel-2 tile, with LAI observations containing only fields with available data within 14 days before or after the simulated anthesis date.

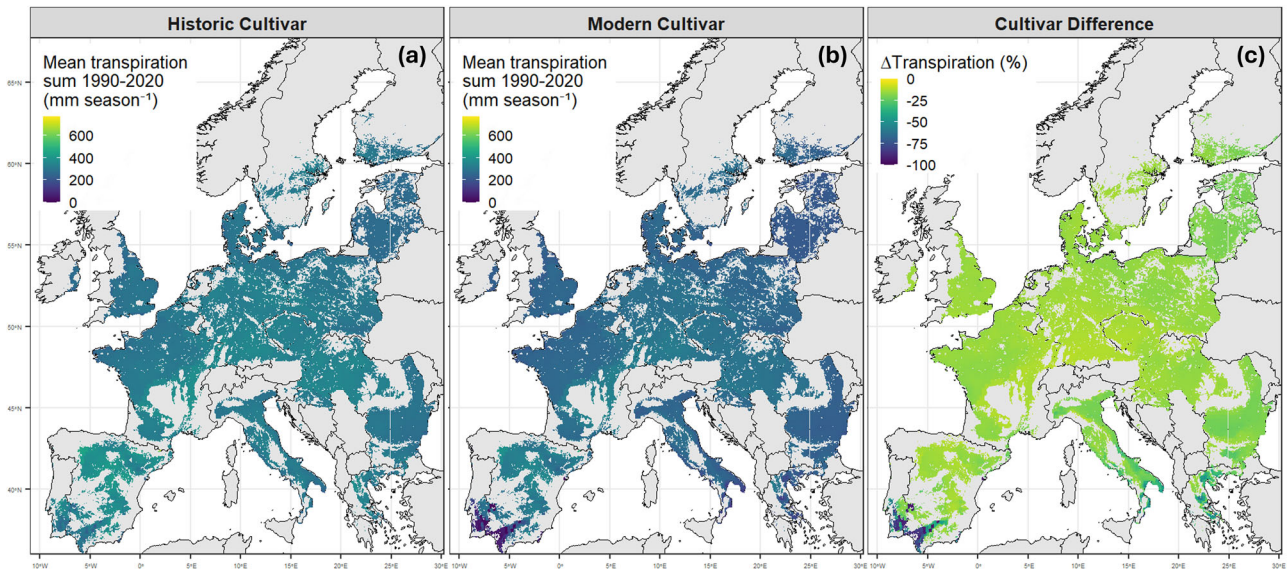

Fig. 4 | Simulation of cultivar transpiration across Europe. Mean transpiration during the growing season for the period of 1990-2020 (mm growing season^{-1}, sowing to harvest) from a crop model simulation of a historic winter wheat cultivar (**a**), modern (**b**), and difference between the modern and historic cultivar relative to the historic cultivar expressed in percentages (negative difference percentage mean larger values for the historic cultivar), **c** over major wheat grown areas in the European Union.

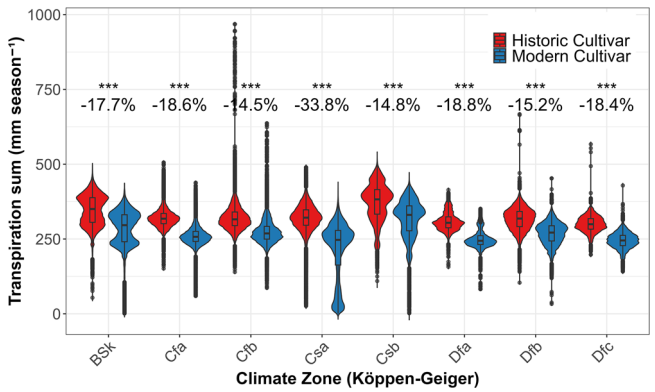

Fig. 5 | Simulated cultivar transpiration for different European climate zones. Boxplots and violin plots of simulations of seasonal transpiration (mm growing season^{-1}, sowing to harvest) from a crop model simulation of a modern (blue) and a historic winter wheat cultivar (red) for the years 1990–2020 in different climate zones. *X*-axis shows climate zones according to the Köppen-Geiger classification by Beck et al.[65]. Stars indicate level of significant differences ($p < 0.001$) between cultivars for each climate zone, calculated using a one-way ANOVA. Numbers (in %) indicate relative differences between cultivars.

are mainly caused by contrasting results in the modern cultivar, where some locations within Csa show very low transpiration sums (i.e. Southern Spain). When comparing simulations within Csa by dividing the locations into subzones based on the available soil water capacity (AWC), locations with the low transpiration sums were associated with a low AWC and low cumulative precipitation during the growing season (Fig. S1). Differences between cultivars in southern Spain can also be observed in the potential transpiration rates in that region (Fig. S2).

When comparing the simulation of the mean yearly transpiration rates of both cultivars during the simulation period, simulations showed a significant trend ($p < 0.001$) in both cultivars towards increasing transpiration rates over time (Fig. 6). With yearly transpiration rates of 352 ± 35 and 293 ± 48 mm for the historic and modern cultivar, respectively. transpiration rates were 15% and 17% larger in the growing season 2019/2020 than in the growing season 1990/1991 with mean yearly transpiration values of 251 ± 44 mm for the modern cultivar and 305 ± 41 mm for the historic cultivar (Fig. 6). The growing season with the smallest difference between the cultivars of −14.8% was the season 2012/2013, largest differences were observed in the season 2001/2002 with −18.5%. Although differences between cultivar slopes over time are small when comparing all locations combined (slope of 0.88 for both), when comparing temporal trends for each climatic zone, some zones showed differences in slopes between

cultivars (Fig. S3), with largest differences between slopes shown in climate zone Csa. Some zones also showed statistically significant trends only for one of the two cultivars, for example with a slope of 0.49, the modern cultivar showed no statistically significant trend of increasing transpiration over time while the historic cultivar did with a slope of 0.55, suggesting a decrease or increase in cultivar differences.

Physiological differences between cultivars

Besides comparing the cultivar differences in transpiration, we also compared differences in maximum LAI, and maximum root hydraulic conductance (d^{-1}) in space and time (Fig. 7). Averaged over the entire region and time, the modern cultivar exhibited significantly lover maximum LAI values of 3.8 ± 0.5 compared to the historical cultivar with values of 5.93 ± 0.37, resulting in a reduction in LAI of $-36.22 \pm 6.68\%$. Similarly, the modern cultivar displayed considerably reduced root hydraulic conductance values (0.00023 ± 0.00013 (d^{-1})) relative to the historical one (0.00127 ± 0.00062 (d^{-1})), a decline of $-82.5 \pm 2.7\%$.

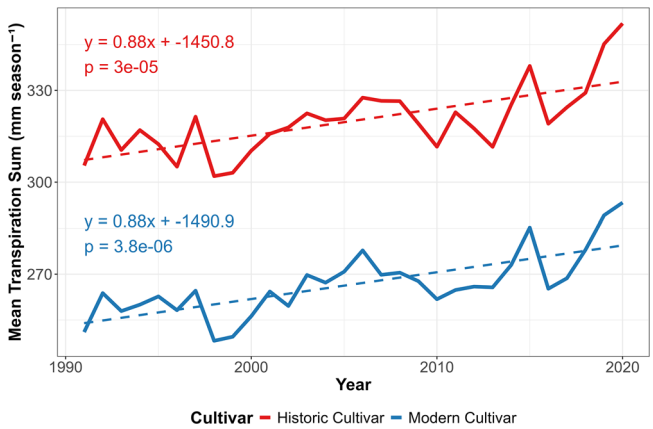

Fig. 6 | Simulated transpiration across Europe from 1990-2020. Mean annual simulated transpiration sum (mm growing season^{-1}, from sowing to harvest) by a crop model simulation of a modern (blue) and a historic (red) winter wheat cultivar for the years 1990–2020 across Europe. Dashed lines show the regression line of a linear mode, with slope and *p* values shown as text.

While differences between the cultivars in LAI and root hydraulic conductivity showed only small variations across the continent, with coefficient of variations of 18.4% for LAI and 3.2% for root hydraulic conductance, differences in aboveground biomass were spatially more variable, showing a coefficient of variation of 386% (Fig. 7). With the modern cultivar accumulating an average of 17.7 ± 3.04 t ha^{-1} vs. 18.13 ± 2.02 t ha^{-1} of the historical cultivar, differences were small ($-2.84\% \pm 10.98\%$). Biomass differences showed both positive and negative values across the domain, indicating that the modern cultivar outperformed the historic cultivar in biomass accumulation at certain locations. This resulted in higher water use efficiencies (WUE; defined as: total aboveground biomass at harvest (kg m^{-2}) divided by transpiration (mm)) in the modern cultivar (Fig. S4). Throughout all locations and years, the modern cultivar showed water use efficiencies that were 16.71% higher than in the historical cultivar.

When plotting the percentage change in the annual cultivar transpiration rate against the percentage change in the physiological variables of maximum LAI, maximum hydraulic conductance (Krs) and day of the year (DOY) of anthesis, all three physiological variables exhibited a highly significant linear relationship ($p < 0.001$; Fig. 8). From the physiological variables compared here, the weakest relationship to differences in transpiration in the two cultivars was phenology, with a coefficient of determination (R^2) of 0.011. With a positive slope, larger differences between cultivars in phenology, so later date of anthesis in the historic cultivar, also result in larger differences in transpiration. The second biggest impact of the compared physiological variables on cultivar differences was related to Krs, with an R^2 of 0.639. Of the compared physiological differences, the biggest R^2 with transpiration rates of the cultivars were observed in LAI with R^2 of 0.871.

When comparing the differences between physiological variables and transpiration of the two cultivars for different climate zones, cultivar reactions differed (Fig. S5). In the climate zone Csa, which is characterized by a temperate climate with a dry and hot summer, root hydraulic conductivity showed a higher R^2 value of 0.844, than in the comparison of the whole domain (Figs. 8 and S5), indicating a higher importance in that climate zone. In the climate zone Dfc, characterized by a cold climate with not dry season and a cold summer, root hydraulic conductivity showed an R^2 value of only 0.215.

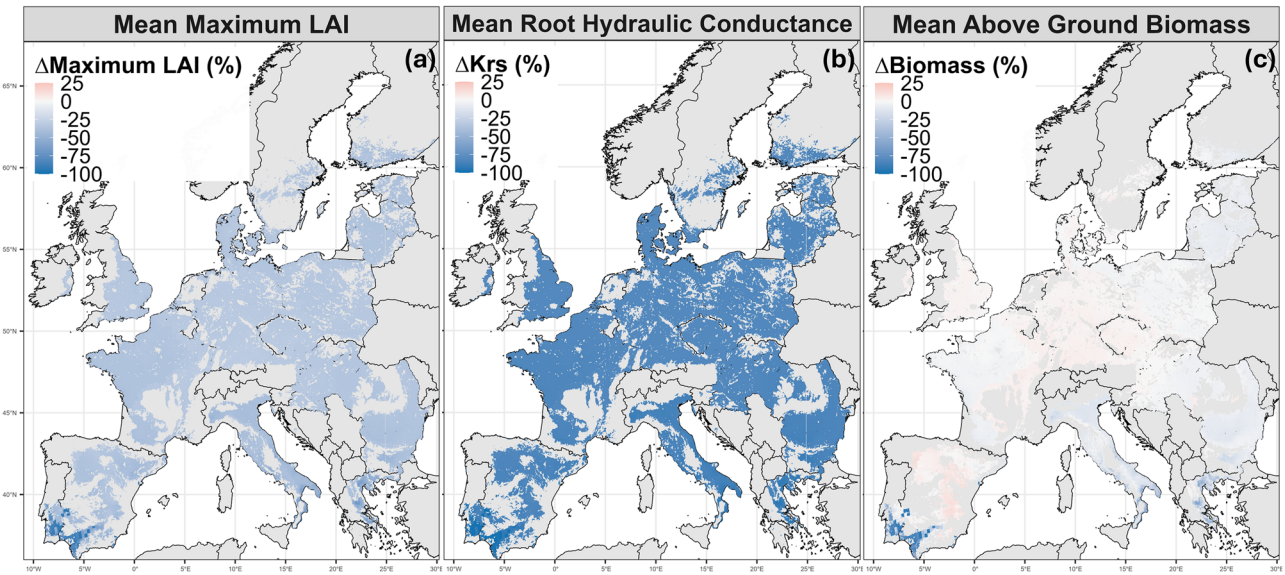

Fig. 7 | Simulated difference in cultivar physiology across Europe. Differences in simulated seasonal maximum LAI (**a**), root hydraulic conductance (**b**) and above ground biomass at harvest (**c**) between a modern and a historic wheat cultivar relative to the historic cultivar over the major wheat grown areas in the European Union for the period of 1990–2020. Positive differences indicate that the respective variable has a greater value for the historic cultivar than for the modern cultivar.

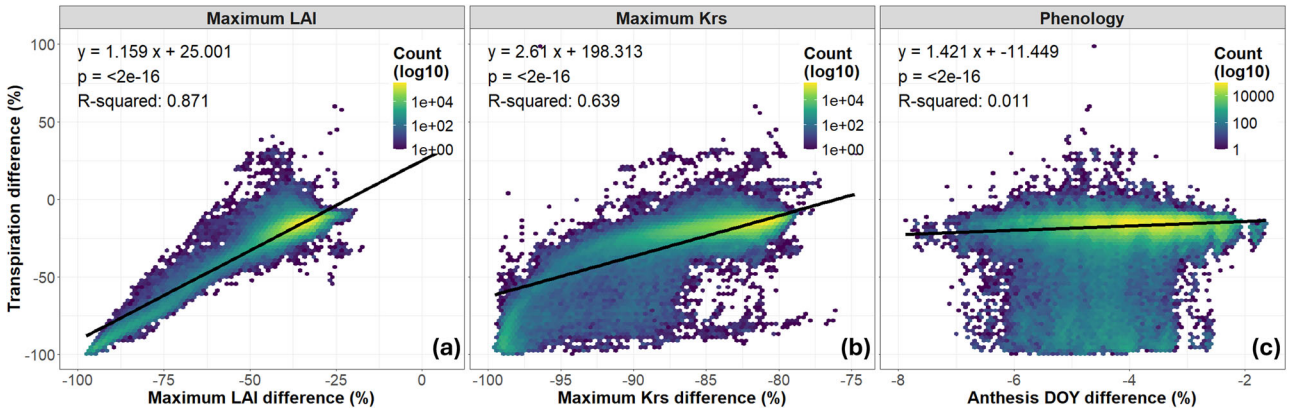

Fig. 8 | Relationship between differences in transpiration and differences in physiology. Relationship between differences in transpiration rates and physiological differences of maximum LAI (**a**), root hydraulic conductance (Krs; **b**) and phenology (**c**) between a modern cultivar and historical cultivar. Colors of hexagons indicate the data density in the respective hexagon over ~5.4 million location-year combinations (European Union; 1990–2020). Black lines and annotations show results of a linear regression.

Discussion

The simulation results indicate that the modern winter wheat cultivar consistently transpires less water over its growing season than the historic cultivar. On average, the modern cultivar used 17% less water (266.5 ± 41.2 vs. 320.2 ± 32.4 (mm m^{-2} growing season^{-1})) than the historical cultivar (Fig. 4). Previously other changes in agricultural management like the consideration of irrigation in land surface models also resulted in significant changes in canopy transpiration. As reported in Sacks et al.[23], the mean daily canopy transpiration increased by 0.579%, averaged over the whole year and all land points. As we are only considering locations across Europe in which winter wheat is commonly grown[36], and winter wheat does not cover the land for the whole year, those results cannot directly be compared. When considering that wheat covers approximately 4% of the European land surface[1], and that winter wheat growing durations throughout all years and locations in our simulations averaged about 286 days, cultivar differences in yearly canopy transpiration sums according to our simulations would result in a difference of approximately 0.53% and would therefore be comparable to the implementation of irrigation as observed by Sacks et al.[23].

Differences between transpiration rates of wheat genotypes align with the results of other studies that investigated differences between transpiration rates and values of genotypes from different origins and grown in different environments[18–20,37]. While transpiring less, the modern cultivar produced similar amounts of above ground biomass (Fig. 7), resulting in a higher water use efficiency (WUE) in our simulations (Fig. S4). Similar results of a higher WUE in modern cultivars was also reported by Siddique et al.[20], which they related to traits such as faster development and a higher harvest index. Those findings suggest that, at least in the case of our two German varieties, breeding-driven gains in yield have not come at the cost of greater water consumption. Differences in transpiration between cultivars were larger in southern European regions and climate zones than in northern climates (Figs. 4 and 6). While differences between cultivars were significant in all climate zones, the biggest differences between cultivars were observed in the climate zone Csa, which is defined as a Mediterranean climate with a dry and hot summer. In our simulation domain, the climate zone Csa can be found in south-west Spain, southern France, south-west Italy and Greece. According to the 30-year mean weather data, those are the regions with the highest temperatures and radiation levels and the lowest precipitation amounts (Fig. S6). Differences were especially pronounced in locations with a low soil available water capacity (Fig. S1). Such interactions between the impact of environmental conditions on the transpiration of different wheat genotypes were previously also reported in by other studies[17,18,37], and seem to become especially pronounced in water-limited environments. Cultivars can differ in their thresholds under which they close their stomata under drought stress or high vapor pressure deficits[37]. Those differences were related by Schoppach et al.[17] with a smaller root metaxylem in winter wheat cultivars with a higher sensitivity to vapor pressure deficits. This reduction in the metaxylem number of modern cultivars was also observed in a recent study by Jones et al.[16], where the root anatomy of the two cultivars used for this simulation study was investigated. In our crop model, this trait is indirectly represented by the difference in the root- and plant hydraulic conductivity, which was the primary parameter used in the calibration of the transpiration rate in this study (Tables S5 and S6). Due to the higher root hydraulic conductivity and the higher number of roots in the historic cultivar Baca Cabrera et al.[15], it can take up water under lower soil water potentials than the modern cultivar, resulting in a delayed transpiration restriction under low water availability. This delayed reaction to low soil water potential increases transpiration over the whole growing season, but it can also cause a faster depletion of water resources, possibly limiting available water resources at later stages of growth, for example during grain filling. A delayed transpiration restriction under low water availability is supported by the linear models used to compare how physiological differences between cultivars affect differences between transpiration rates (Fig. 8). Means throughout all environments and years, show a coefficient of determination (R^2) of the difference in root hydraulic conductance to the difference in transpiration of 0.639 (Fig. 8), looking only at the climate zone Csa, this R^2 is bigger with a value of 0.844 (Fig. S5). These results highlight that differences between genotypes in their water use are dependent on their environment and can become especially pronounced in water limited, high demanding environments.

While transpiration differences between cultivars in the dry regions seem to be mainly correlated to root traits, crop physiological properties related to transpiration differences across the domain seem to involve both canopy and root system traits (Fig. 8). All traits compared in this study, namely phenology, maximum seasonal LAI and seasonal maximum root hydraulic conductance affected the difference between cultivar transpiration rates significantly. While the effect of phenology on transpiration was significant, phenological differences between cultivars in our modeling experiment were mainly related to differences in anthesis timings, which resulted from the fact that harvests in our experiment were performed at the same time. Other studies however also reported differences in the date of maturity between historic and modern varieties[38], which would likely impact the results and increase differences further. The largest impacts on the differences in transpiration between the cultivars was maximum LAI with an R^2 value of 0.871. Similarly to the results of the field experiments, LAI values were

larger in the historical cultivar throughout most times and locations in of our simulations (Fig. 7).

Besides the differences in space, our results show a significant increase in yearly transpiration sum in both cultivars with the year of the simulation. Percentual increases from the season of 1990/1991 to the season 2019/2020 were 15% for the historic cultivar and 17% for the modern cultivar (Fig. 6). This trend can likely be attributed mainly to rising temperatures and higher solar radiation within the simulated period (Fig. S7). Warmer air can hold more moisture and drives up vapor pressure deficits, together with greater net radiation this boosts evaporative demand and plant potential transpiration[39].

This trend of increasing transpiration sums in both cultivars is despite increasing CO_2 concentrations. Elevated CO_2 can improve WUE in plants, due to a reduction in the stomata conductance[40,41]. While the stomatal conductance model used in our simulations does consider the direct effect of elevated CO_2 concentrations on stomatal conductance[42], it does not consider an acclimation effect that occurs with increasing CO_2 concentrations, such as a reduced Rubisco content, and that is likely to have even a greater water saving effect[40]. Such an acclimation effect might only be properly considered, when calibrating the model with data under elevated conditions such as free-air CO_2 enrichment experiments.

When looking at temporal trends in transpiration rates in different climate zones, transpiration rates seemed to increase faster in warm regions than in colder regions, with slopes of the linear models being the lowest in the regions, Csa, Csb and Cfa (Fig. S3). These differences in trends between the climatic zones are likely caused by differences in changes of climatic factors during the simulation duration. When comparing the trend in changes of environmental variables over the period between the zone with the biggest regression slope in transpiration over the simulated period Dfb, with the zone that showed the lowest slope Cfa, both zones showed a significant increase in temperature sums and VPD with the simulated year, but only Dfc also showed a significant increase in radiation (Fig. S8). This trend in rising plant transpiration with time is expected to continue with climate change and emphasizes the importance of developing winter wheat cultivars with better WUE to maintain yield resilience under a warming climate.

It should be noted that our upscaling approach includes necessary assumptions, that might significantly affect outcomes of transpiration rates, for example do other management changes also affect feedbacks between atmosphere and croplands and likely interact with the cultivar grown, like the fertilizers applied, irrigation and sowing and harvesting dates chosen[3,4,8,30,34]. We further had to make cultivar specific assumptions in both space and time. While the two cultivars represent common winter wheat cultivars in their time of release in German, we want to highlight that those two cultivars alone are not enough to represent general breeding trends, which requires experiments with large cultivar panels. The only spatial difference between the cultivar physiology we could implement was in phenology. While we managed to adapt the database by Ceglar et al.[43] with regards to phenology, other physiological traits, like the LAI or root water uptake might also differ in space (for example cultivars grown in the Mediterranean might have even a better WUE than the modern cultivar investigated here). This highlights the need of a database with functional crop traits for simulations.

Our simulations show that breeding related physiological differences between winter wheat cultivars can significantly affect transpiration across Europe. On average, the modern cultivar transpired 17% less water than the historic cultivar in our simulations. These differences between cultivars were spatially heterogeneous showing larger differences in Mediterranean regions, and temporally variable, with both cultivars showing an overall increase in seasonal transpiration between 1990 to 2020. The magnitude of these cultivar effects is comparable to other management impacts on transpiration, like the use of irrigation. Considering the importance of wheat as a land cover in Europe, our findings suggests that genetic improvements in crops might alter continental water cycles and should not be neglected in land surface models.

While this study provides a first large-scale assessment of cultivar impacts on transpiration, limitations remain. Only two cultivars were compared, and shifts in other management practices were not explicitly addressed. Future studies should expand to multiple cultivars and trait databases and should evaluate how cultivar-driven transpiration differences evolve under future climate scenarios. Overall, our findings emphasize the need to integrate cultivar specific model parameters into land surface models, as breeding-induced changes in physiology not only affect yield but also shape water fluxes between croplands and the atmosphere.

Materials and methods

Crop model description

Simulations were performed using the process-based crop growth model SIMPLACE < HILLFLOW -1D-Couvreur RWU – SlimRoot - LintulCC2> (LintulCC2), implemented as a model solution within the modeling framework SIMPLACE[31]. The model uses the physically-based soil water balance model HILLFLOW, that calculates water fluxes by numerically solving the Richards equation[44]. Root water uptake is described using the one-dimensional model[45] that simulates root water uptake using a water potential gradient-based approach, in which the root system hydraulic conductance is calculates as a function of the root length density:

$$K_{rs,doy} = K_{rs,normalized} * TRLD_{doy} \quad (1)$$

Where $K_{rs,doy}$ (d^{-1}) is the root hydraulic conductance, $K_{rs,normalized}$ ($d^{-1}\,cm^{-1}\,m^2$) is the root system conductance per unit root length per surface area and $TRLD_{doy}$ is the total root length density below a unit surface area ($m\,m^{-2}$). Root growth is simulated using the SIMPLACE component SlimRoots[46]. Crop growth is simulated using the crop model LintulCC2[32,47]. LintulCC2 simulates photosynthesis using the model proposed by Farquhar et al.[48] and Farquhar and von Caemmerer[49], using the stomatal conductance model by Leuning[42]. A schematic overview of the crop model can be found in Fig. S9. A more detailed description of the model and its processes can be found in Nguyen et al.[32].

To upscale the model to the continental scale, a dataset that contains information about phenological temperature sum requirements was used[43]. This required an adaptation of the phenology component of the original model used by Nguyen et al.[32] to consider the effects of vernalization and photoperiod, as used in Ceglar et al.[43], which was based on Porter[50] and Ewert et al.[51]:

$$DVS = \begin{cases} \sum_i \frac{max\left(0, min\left(\left(T_i - T_b\right), T_{max,e}\right)\right)}{TSUM_1} * V_{f,i} * P_{f,i} \; for \; DVS \le 1 \\ \sum_i \frac{max\left(0, min\left(\left(T_i - T_b\right), T_{max,e}\right)\right)}{TSUM_1} \; for \; 1 < DVS \le 2 \end{cases} \quad (2)$$

Where DVS represents the developmental stage of the crop as an index from 0 (emergence) to 2 (physiological maturity), T_i the daily average temperature (°C), T_b the base temperature (here always considered to be 0 °C), $T_{\max,e}$ the maximum effective temperature above which the developmental rate remains constant (here considered to be 30 °C), $TSUM_1$ the temperature sum required until anthesis, $V_{f,i}$ the vernalization factor and $P_{f,i}$ the photoperiod factor on day i. The photoperiod factor is calculated as:

$$P_{f,i} = \begin{cases} \frac{P_i - P_b}{P_{opt} - P_b} for \; P_b \le P_i \le P_{opt} \\ 1 \; for \; P_i > P_{opt} \\ 0 \; for \; P_i < P_b \end{cases} \quad (3)$$

where P_i ($h\,d^{-1}$) is the daily photoperiod, P_b ($h\,d^{-1}$) is the base photoperiod below for which no development is observed (here always considered to be 8) and P_{opt} ($h\,d^{-1}$) is the optimum photoperiod, assumed to take a value of the local maximum day length occurring on the 21st of June according to[52].

The vernalization factor was calculated as:

$$V_{f,i} = \begin{cases} 0 \, for \, V_{DD} < V_b \\ \frac{V_{DD} - V_b}{V_{sat} - V_b} \, for \, V_b \le V_{DD} \le V_{sat} \\ 1 \, for \, V_{DD} > V_{sat} \ \vee \ DVS > 0.3 \end{cases} \quad (4)$$

where V_{DD} is the accumulated effective vernalized days from emergence onwards, V_{sat} represents the saturated vernalization requirements and V_b is the base accumulated vernalized days. All parameter values were chosen to be equal to the ones suggested by Ceglar et al.[43].

Additional to the changes in the phenology model, the biomass partitioning routine was adapted as a preparation for the upscaling. Previously, biomass partitioning between plant organs was simulated using interpolation tables consisting of partitioning fractions for each organ depending on the accumulated temperature sum. Those interpolation tables were kept, and partitioning fractions were made dependent on the developmental stage of the crop instead of the accumulated temperature sum.

Experimental data and model calibration

Crop model calibration was performed using data of a field experiment with two consecutive growing seasons (2022/2023 and 2023/2024) at Campus Klein-Altendorf, near Bonn, Germany (50°37' N, 6°59' E). Information about the experimental management and the measurements taken relevant to the model calibration can be found in Supplementary Materials Section 1—"Experimental overview" and Table S1. A detailed description of the experimental setup and the conducted measurements can be found in Behrend et al.[35]. Out of the 6 cultivars investigated in Behrend et al.[35], the two varieties with the largest gaps between their year of release were chosen for the simulations presented here, Tommi (released 2002) and S. Dickkopf (released 1895). For the model calibration, data of the experimental season 2023–2024 was used, for validation, data of the experimental season 2022–2023 was used. Data used for model calibration previously discussed in Behrend et al.[35] includes data about cultivar phenology, LAI, biomass partitioning between leaf, stem, root and grain, and data about the total biomass. Besides the data discussed in Behrend et al.[35], transpiration measurements were conducted using sap flow sensors, only during the experimental season 2023–2024 and model calibration. For each cultivar, 5 sap flow sensors (SAG3; Dynamax Inc., Houston USA) were installed on 27.05.2024, when the stem diameters where large enough. Data collection was done using a CR1000 data logger and two AM 16/32 multiplexers (Campbell Scientific, Logan, Utah USA). Vertical and temperature gradients within each sensor were recorded at 10-min intervals and later aggregated to hourly intervals. Temperature gradients were then used to calculate sap flow according to Langensiepen et al.[53]. Upscaling of the measurements from the transpiration rates of each tiller (g h^{-1}) to the canopy transpiration rates (mm h^{-1}) was performed using the mean tiller number of the respective cultivar measured at installation of the sensors and before harvest[35]. For the calibration of the model, measured daily transpiration sums were used (mm d^{-1}).

Both cultivars were represented by the same model structure. Model calibration was performed for both cultivars individually, according to the crop model calibration protocol by Wallach et al.[54]. Tables suggested by Wallach et al.[54], including information about the parameters, their values before and after the calibration and a description of the algorithms used for the calibration can be found in the Supplementary Materials Section S2—"Crop model calibration". The experiment was performed under the maximum possible nitrogen fertilization rates in its region, with the help of chemical weed and pest and disease control and under rainfed conditions. For both the model calibration at the field scale and the upscaling, optimal management conditions with regards to nutrients, weeds and pest and diseases pressure, as present in the field experiment, as well as rainfed conditions were assumed.

Model validation was performed using the root mean squared error (RMSE):

$$RMSE = \sqrt{\frac{\sum (y_i - \hat{y}_i)^2}{n}} \quad (5)$$

where y_i is the ith measurement and $\hat{y}_i$ the corresponding simulated variable value. Besides the RMSE, evaluation of model fit was performed using the relative RMSE (rRMSE):

$$rRMSE = \frac{RMSE}{\bar{y}} \quad (6)$$

where $\bar{y}$ is the mean of the observed values, the Mean Absolute Error (MAE):

$$MAE = \frac{1}{n} \sum |y_i - \hat{y}_i| \quad (7)$$

And the Willmott's Index of Agreement (d-index), which is a measure of model fit with optimal values close to 1 is calculated as follows:

$$d - index = 1 - \frac{\sum (\hat{y}_i - y_i)^2}{\sum \left(|\hat{y}_i - \bar{y}| + |y_i - \bar{y}| \right)^2} \quad (8)$$

Upscaling to the continental scale

The upscaling to the European continental scale was done within the domain of the Coordinated Regional Down-scaling Experiment (CORDEX)[55,56], on a 3 by 3 km resolution. To reduce the number of simulations, while still covering the main wheat growing areas across the European Union, locations used for the simulations were filtered from the CORDEX domain, based on a recent probabilistic crop type map for the European Union[36]. The crop type map contains yearly probabilities for several crop types from 1990 to 2018 on a 1 km grid. The map was first adjusted to the coordinate reference system and resolution of the domain using bilinear interpolation from the function "project" of the R package "terra"[57], and then averaged over the whole period. All grid cells for which the average probability of soft and durum wheat being cultivated exceeds 5% were chosen for the simulation. This resulted in a total number of 180,934 grid cells or 19.5%, from a total of 928.655 cells over land.

Weather and soil input data

As weather input data, the hourly ERA5-reanalysis dataset was used for the years 1990–2020[58], which corresponds to the simulation period. Similarly to the crop type map, the ERA5-reanalysis data was bilinearly remapped to the 3 km grid.

To reduce the amount of input data, CO_2 concentrations in the air were input separately from the other weather variables to the model using globally averaged marine surface annual mean data[59]. Information about the average altitude of the grid cells was obtained from the Copernicus digital elevation model[60].

Soil texture variables, as well as bulk density and soil organic matter fractions used were obtained from the SoilGrids 2.0 database and also remapped[61]. Soil hydraulic properties of the respective soils were further calculated using the Hydraulic Properties of European Soils (HYPRES) pedotransfer functions[62]. Soil moisture levels at the beginning of the simulated period were set to field capacity.

Phenology, sowing and harvesting dates

To account for spatial differences in the phenology of winter wheat cultivars across Europe, phenological model parameters obtained from the dataset of Ceglar et al.[43] were used for simulations of the modern cultivar Tommi. The dataset contains information about sowing dates, temperature sums from

sowing to anthesis and temperature sums from anthesis to harvest, obtained with the help of an agro-phenological database as described in Ceglar et al.[43].

Phenology of the historic cultivar was adapted according to the mean observations from the two-year field experiment, where differences between the phenological development of the historic and modern cultivars were observed, with temperature sums from sowing to anthesis being 12% higher and temperature sums from anthesis to maturity being 11% lower in the historic cultivar. The temperature sums from sowing to anthesis obtained by Ceglar et al.[43] for the simulations of the historic cultivar where therefore adapted by multiplying it with a factor of 1.12, while temperature sums from anthesis to maturity were multiplied by 0.89 across the whole domain. Thermal time requirements from sowing to anthesis of modern and historic cultivars are visualized in Fig. S10. Harvest dates of both cultivars were chosen based on their physiological maturity. Sowing dates of both cultivars were the ones suggested by Ceglar et al.[43].

Leaf area index observations for validation

Validation of the continental simulations was done using remotely sensed green leaf area index (GLAI) data obtained from Sentinel-2 with a 10 × 10 m spatial resolution at a 5–15 days interval, for several locations in countries across Europe (Germany, Italy, Romania, Spain and the UK) during the growing seasons from 2017–2020, previously used and described by Nguyen et al.[33]. Locations were chosen, based on known exact locations of wheat fields and consisted of 30 fields per year, and Sentinel-2 tile. GLAI was computed using the Sentinel Application Platform (SNAP v 8.0) using an approach by Weiss et al.[63], as described in Nguyen et al.[33]. Observations were compared with simulations of the LAI at the date of anthesis of the modern cultivar. Only observations within a time window of 14 days before or after the simulated date of anthesis were chosen for comparisons. Dates were further filtered by the number of observations per date and tile. Due to cloud cover, valid observations per date and tile varied, only dates with information for more than 50% of the fields were chosen for the comparison. As no information about the actual cultivar grown on these fields was available, comparisons were performed with simulation results of the model calibrated with data of the modern cultivar Tommi.

Data analysis

Cultivar transpiration was calculated for each growing season, from sowing to harvest. Mean cultivar differences in transpiration over the 30-year timespan were evaluated using one-way analysis of variance (ANOVA). To capture spatial interactions between grown cultivars and the environment, the simulation domain was divided into different climate classes according to the Köppen-Geiger classification[64], using a dataset by Beck et al.[65]. The climate zones present in the domain are: BSk (Arid, steppe, cold), Csa (Temperate, dry summer, hot summer), Csb (Temperate, dry summer, warm summer), Cfa (Temperate, no dry season, hot summer), Cfb (Temperate, no dry season, warm summer), Dfa (Cold, no dry season, hot summer), Dfb (Cold, no dry season, warm summer), Dfc (Cold, no dry season, cold summer). The number of grid cell locations within each climate zone, are depicted in Fig. S11. To further investigate spatial variability in modeled transpiration sums within the Csa climate zone, an additional stratified analysis was conducted. Within the Csa climate zone, grid cell locations were stratified into three available water capacity (AWC) classes based on the distribution of soil available water capacity. AWC was calculated as the depth-weighted mean difference between soil water content at field capacity and at permanent wilting point across the soil profile. For each soil layer, the difference between field capacity and wilting point was multiplied by layer thickness, summed over all layers, and normalized by the total soil profile depth. The lowest and highest quartiles of AWC were classified as low and high AWC, respectively, while the interquartile range represented medium AWC. The resulting AWC classes covered ranges of 0.083–0.106, 0.106–0.116, and 0.116–0.208 (%), respectively.

Temporal trends in cultivar transpiration due to temporal changes in weather variables were calculated using a linear regression model with transpiration rate as response variable and the year of simulation as predictor. Linear regression models were also used to assess the impact of differences between cultivars in simulated physiological variables like LAI, root hydraulic conductance and phenology on the simulated difference in transpiration across Europe. The impact of climate and soil variables on the cultivar transpiration was estimated using linear mixed-effects models using the R package 'lme4'[66]. Before fitting the model, climate variables used as predictors were normalized to zero mean and unit variance:

$$X_{normalized} = \frac{X - \bar{X}}{\sigma(x)} \tag{9}$$

where $\bar{X}$ is the sample mean and $\sigma(x)$ the standard deviation across all observations. To quantify how cultivar-driven differences in physiological variables explain differences in season transpiration patterns, a linear mixed effects model was applied, adding the Köppen-Geiger climate zone as a random intercept. All predictors of the mixed effects model were normalized to allow an easier comparison.

Data availability

The data of the simulation outputs used in this manuscript are uploaded and are freely accessible on the bonndata repository (https://doi.org/10.60507/FK2/QCZ9KA).

Code availability

Source code of the model used for the simulation and detailed documentation are freely accessible on the SIMPLACE homepage: https://www.simplace.net/. Code to post-process the model outputs, generate figures, and process the weather and soil input data is published together with the model output data on the bonndata repository (https://doi.org/10.60507/FK2/QCZ9KA).

Received: 10 November 2025; Accepted: 27 January 2026;
Published online: 31 March 2026

References

1. Eurostat. Land cover in the EU. (2022).
2. Pinke, Z. et al. Climate change and modernization drive structural realignments in European grain production. *Sci. Rep.* **12**, 7374 (2022).
3. Ahrends, H. E. et al. Genetic yield gains of winter wheat in Germany over more than 100 years (1895–2007) under contrasting fertilizer applications. *Environ. Res. Lett.* **13**, 104003 (2018).
4. Rezaei, E. E. et al. A tale of two eras: assessing the impact of breeding programs on historical and modern German wheat cultivars under distinct management. *Eur. J. Agron.* **156**, 127179 (2024).
5. Wang, T.-C. et al. Multi-environment field trials for wheat yield, stability and breeding progress in Germany. *Sci. Data* **12**, 64 (2025).
6. Reynolds, M. et al. Raising yield potential in wheat. *J. Exp. Bot.* **60**, 1899–1918 (2009).
7. Foulkes, M. J. et al. Raising yield potential of wheat. III. Optimizing partitioning to grain while maintaining lodging resistance. *J. Exp. Bot.* **62**, 469–486 (2011).
8. Rezaei, E. E., Siebert, S., Hüging, H. & Ewert, F. Climate change effect on wheat phenology depends on cultivar change. *Sci. Rep.* **8**, 4891 (2018).
9. Rose, T. & Kage, H. The contribution of functional traits to the breeding progress of Central-European winter wheat under differing crop management intensities. *Front. Plant Sci.* **10**, 1521 (2019).
10. Kumar, P. et al. Characterization of flag leaf morphology identifies a major genomic region controlling flag leaf angle in the US winter wheat (Triticum aestivum L.). *Theor. Appl. Genet.* **137**, 205 (2024).
11. Voss-Fels, K. P., Snowdon, R. J. & Hickey, L. T. Designer roots for future crops. *Trends Plant Sci.* **23**, 957–960 (2018).
12. Fang, Y. et al. Moderate drought stress affected root growth and grain yield in old, modern and newly released cultivars of winter wheat. *Front. Plant Sci.* **8**, 672 (2017).

13. Friedli, C. N., Abiven, S., Fossati, D. & Hund, A. Modern wheat semi-dwarfs root deep on demand: response of rooting depth to drought in a set of Swiss era wheats covering 100 years of breeding. *Euphytica* **215**, 85 (2019).
14. Fradgley, N. et al. Effects of breeding history and crop management on the root architecture of wheat. *Plant Soil* **452**, 587–600 (2020).
15. Baca Cabrera, J. C. et al. Decreased root hydraulic traits in German winter wheat cultivars over 100 years of breeding. *Plant Physiol.* **198**, 166 (2025).
16. Jones, D. H. et al. The Rapid Anatomics Tool (RAT): a low-cost root anatomical phenotyping pipeline reveals changes in root anatomy along the root axis. *bioRxiv* **09**, 674482 (2025).
17. Schoppach, R., Wauthelet, D., Jeanguenin, L. & Sadok, W. Conservative water use under high evaporative demand associated with smaller root metaxylem and limited trans-membrane water transport in wheat. *Funct. Plant Biol.* **41**, 257–269 (2013).
18. Moritz, A., Eckert, A., Vukasovic, S., Snowdon, R. & Stahl, A. Physiological phenotyping of transpiration response to vapour pressure deficit in wheat. *BMC Plant Biol.* **24**, 1032 (2024).
19. Huang, G. et al. Plant architecture influences the population transpiration and canopy temperature in winter wheat genotypes. *Agronomy* **13**, 742 (2023).
20. Siddique, K., Tennant, D., Perry, M. & Belford, R. Water use and water use efficiency of old and modern wheat cultivars in a Mediterranean-type environment. *Aust. J. Agric. Res.* **41**, 431 (1990).
21. McDermid, S. et al. Irrigation in the Earth system. *Nat. Rev. Earth Environ.* **4**, 435–453 (2023).
22. Yang, Z. et al. Impact of irrigation over the California Central Valley on regional climate. *J. Hydrometeorol.* **18**, 1341–1357 (2017).
23. Sacks, W. J., Cook, B. I., Buenning, N., Levis, S. & Helkowski, J. H. Effects of global irrigation on the near-surface climate. *Clim. Dyn.* **33**, 159–175 (2009).
24. Chen, M. et al. Comparing crop growth and carbon budgets simulated across AmeriFlux agricultural sites using the Community Land Model (CLM). *Agric. For. Meteorol.* **256–257**, 315–333 (2018).
25. Kucharik, C. J. & Brye, K. R. Integrated biosphere simulator (IBIS) yield and nitrate loss predictions for Wisconsin maize receiving varied amounts of nitrogen fertilizer. *J. Environ. Qual.* **32**, 247–268 (2003).
26. Oleson, K. W. et al. Technical description of version 4.5 of the Community Land Model (CLM). Tech. Descr. Version 45 Community Land Model CLM2013 NCARTN-503 STR 503, (2013).
27. Osborne, T. et al. JULES-crop: a parametrisation of crops in the Joint UK Land Environment Simulator. *Geosci. Model Dev.* **8**, 1139–1155 (2015).
28. Sulis, M. et al. Incorporating a root water uptake model based on the hydraulic architecture approach in terrestrial systems simulations. *Agric. For. Meteorol.* **269–270**, 28–45 (2019).
29. Boas, T. et al. Improving the representation of cropland sites in the Community Land Model (CLM) version 5.0. *Geosci. Model Dev.* **14**, 573–601 (2021).
30. Rabin, S. S., Sacks, W. J., Lombardozzi, D. L., Xia, L. & Robock, A. Observation-based sowing dates and cultivars significantly affect yield and irrigation for some crops in the Community Land Model (CLM5). *Geosci. Model Dev.* **16**, 7253–7273 (2023).
31. Enders, A. et al. SIMPLACE—a versatile modelling and simulation framework for sustainable crops and agroecosystems. *Silico Plants* **5**, diad006 (2023).
32. Nguyen, T. H. et al. Comparison of root water uptake models in simulating CO2 and H2O fluxes and growth of wheat. *Hydrol. Earth Syst. Sci.* **24**, 4943–4969 (2020).
33. Nguyen, T. H. et al. Assessing the spatio-temporal tropospheric ozone and drought impacts on leaf growth and grain yield of wheat across Europe through crop modeling and remote sensing data. *Eur. J. Agron.* **153**, 127052 (2024).
34. Hernández-Ochoa, I. M., Gaiser, T., Hüging, H. & Ewert, F. Yield components and yield quality of old and modern wheat cultivars as affected by cultivar release date, N fertilization and environment in Germany. *Field Crops Res.* **302**, 109094 (2023).
35. Behrend, D. et al. Biomass partitioning and canopy architecture of six German winter wheat cultivars released between 1895 and 2002. Preprint at https://doi.org/10.22541/essoar.175822260.03180911/v1 (2025).
36. Baumert, J., Heckelei, T. & Storm, H. A dataset of yearly probabilistic crop type maps for the EU from 1990 to 2018. *Data Brief* **60**, 111472 (2025).
37. Schoppach, R. & Sadok, W. Differential sensitivities of transpiration to evaporative demand and soil water deficit among wheat elite cultivars indicate different strategies for drought tolerance. *Environ. Exp. Bot.* **84**, 1–10 (2012).
38. Bai, H., Tao, F., Xiao, D., Liu, F. & Zhang, H. Attribution of yield change for rice-wheat rotation system in China to climate change, cultivars and agronomic management in the past three decades. *Clim. Change* **135**, 539–553 (2016).
39. Kirschbaum, M. U. F. & McMillan, A. M. S. Warming and Elevated CO2 Have Opposing Influences on Transpiration. Which is more Important? *Curr. For. Rep.* **4**, 51–71 (2018).
40. Ainsworth, E. A. & Long, S. P. What have we learned from 15 years of free-air CO2 enrichment (FACE)? A meta-analytic review of the responses of photosynthesis, canopy properties and plant production to rising CO2. *New Phytol.* **165**, 351–372 (2005).
41. Baca Cabrera, J. C., Hirl, R. T., Schäufele, R., Macdonald, A. & Schnyder, H. Stomatal conductance limited the CO2 response of grassland in the last century. *BMC Biol.* **19**, 50 (2021).
42. Leuning, R. A critical appraisal of a combined stomatal-photosynthesis model for C3 plants. *Plant Cell Environ.* **18**, 339–355 (1995).
43. Ceglar, A. et al. Improving WOFOST model to simulate winter wheat phenology in Europe: evaluation and effects on yield. *Agric. Syst.* **168**, 168–180 (2019).
44. Bronstert, A. & Plate, E. J. Modelling of runoff generation and soil moisture dynamics for hillslopes and micro-catchments. *J. Hydrol.* **198**, 177–195 (1997).
45. Couvreur, V., Vanderborght, J., Beff, L. & Javaux, M. Horizontal soil water potential heterogeneity: simplifying approaches for crop water dynamics models. *Hydrol. Earth Syst. Sci.* **18**, 1723–1743 (2014).
46. Addiscott, T. M. & Whitmore, A. P. Simulation of solute leaching in soils of differing permeabilities. *Soil Use Manag.* **7**, 94–102 (1991).
47. Rodriguez, D. et al. Modelling the response of wheat canopy assimilation to atmospheric CO_2 concentrations. *New Phytol.* **150**, 337–346 (2001).
48. Farquhar, G. D., von Caemmerer, S. & Berry, J. A. A biochemical model of photosynthetic CO2 assimilation in leaves of C3 species. *Planta* **149**, 78–90 (1980).
49. Farquhar, G. D. & von Caemmerer, S. Modelling of photosynthetic response to environmental conditions. in *Physiological Plant Ecology II: Water Relations and Carbon Assimilation* (eds Lange, O. L., Nobel, P. S., Osmond, C. B. & Ziegler, H.) 549–587 (Springer, 1982).
50. Porter, J. R. AFRCWHEAT2: a model of the growth and development of wheat incorporating responses to water and nitrogen. *Eur. J. Agron.* **2**, 69–82 (1993).
51. Ewert, F., Porter, J. & Honermeier, B. Use of AFRCWHEAT2 to predict the development of main stem and tillers in winter triticale and winter wheat in North East Germany. *Eur. J. Agron.* **5**, 89–103 (1996).
52. van Bussel, L. G. J., Stehfest, E., Siebert, S., Müller, C. & Ewert, F. Simulation of the phenological development of wheat and maize at the global scale. *Glob. Ecol. Biogeogr.* **24**, 1018–1029 (2015).
53. Langensiepen, M., Kupisch, M., Graf, A., Schmidt, M. & Ewert, F. Improving the stem heat balance method for determining sap-flow in wheat. *Agric. For. Meteorol.* **186**, 34–42 (2014).

54. Wallach, D. et al. A calibration protocol for soil-crop models. *Environ. Model. Softw.* **180**, 106147 (2024).
55. Giorgi, F., Jones, C. & Asrar, G. R. Addressing climate information needs at the regional level: the CORDEX framework. (2009).
56. Gutowski, W. J. Jr. et al. WCRP COordinated Regional Downscaling EXperiment (CORDEX): a diagnostic MIP for CMIP6. *Geosci. Model Dev.* **9**, 4087–4095 (2016).
57. Hijmans, R. terra: Spatial Data Analysis. (2025).
58. Hersbach, H. et al. ERA5 hourly data on single levels from 1940 to present. Copernicus Climate Change Service (C3S) Climate Data Store (CDS). https://doi.org/10.24381/cds.adbb2d47 (2023).
59. Lan, X., Tans, P. & Thoning, K. W. Trends in globally-averaged CO2 determined from NOAA Global Monitoring Laboratory measurements. https://doi.org/10.15138/9N0H-ZH07 (2025).
60. Copernicus Data Space. Copernicus DEM—Global and European Digital Elevation Model. https://doi.org/10.5270/ESA-c5d3d65 (2019).
61. Poggio, L. et al. SoilGrids 2.0: producing soil information for the globe with quantified spatial uncertainty. *Soil* **7**, 217–240 (2021).
62. Wösten, J. H. M., Lilly, A., Nemes, A. & Le Bas, C. Development and use of a database of hydraulic properties of European soils. *Geoderma* **90**, 169–185 (1999).
63. Weiss, M., Baret, F. & Jay, S. S2ToolBox Level 2 Products: LAI, FAPAR, FCOVER. (Version 2.0). Avignon Inst Natl Rech Agron 53 (2020).
64. Köppen, W. Das geographische System der Klimate (1936). *Gebrüder Borntraeger* **1**, 44 (1936).
65. Beck, H. E. et al. Present and future Köppen-Geiger climate classification maps at 1-km resolution. *Sci. Data* **5**, 180214 (2018).
66. Bates, D., Mächler, M., Bolker, B. & Walker, S. Fitting linear mixed-effects models using lme4. *J. Stat. Softw.* **67**, 1–48 (2015).

Acknowledgements

The authors gratefully acknowledge access to the Bonna High Performance Computing cluster of the University of Bonn.

Author contributions

Conceptualization: D.B., T.H.N., and T.G.; Data curation: D.B.; Formal analysis: D.B.; Funding acquisition: G.L., J.V., F.E., and T.G.; Investigation: D.B.; Methodology: D.B., T.H.N., and T.G.; Software: D.B.; Supervision: T.H.N. and T.G.; Validation: D.B.; Visualization: D.B.; Writing original draft: D.B.; Writing review and editing: D.B., T.H.N., J.C.B.C., J.B., C.O.G.B., D.H.J., G.L., S.J.S., A.S., H.S., J.V., F.E., and T.G.

Funding

Open Access funding enabled and organized by Projekt DEAL.

Competing interests

The authors declare no competing interests.

Additional information

Supplementary information The online version contains supplementary material available at https://doi.org/10.1038/s44264-026-00135-y.

Correspondence and requests for materials should be addressed to Dominik Behrend.